



## **AEROACOUSTIC ASSESSMENT OF LEADING EDGE BUMPS IN INDUSTRIAL FANS**

*Alessandro CORSINI<sup>1</sup>, Giovanni DELIBRA<sup>1</sup>,  
Franco RISPOLI<sup>1</sup> and Anthony G. SHEARD<sup>2</sup>*

*<sup>1</sup> Sapienza University of Rome, Dept. of Mechanical and Aerospace  
Engineering, Via Eudossiana 18, 00184 Roma, Italy*

*<sup>2</sup> Fläkt Woods Limited, Axial Way, Colchester, CO4 5AR UK*

### **SUMMARY**

*Stall control is a key technology for industrial fans. In tunnel and metro applications this technologies are regarded as a key assets, as regulatory and operational conditions limit the viable design choices. In an ongoing investigation we are assessing the stall control capabilities of biomimicry-derived sinusoidal leading edges. In the present paper we focus on the prediction of acoustic emissions of blades with sinusoidal leading edges and compare the acoustic performance with that of the datum blade with straight leading edge. To this aim we performed URANS calculation with the non-linear low-Reynolds model of Lien et al. and applied SPL prediction from Fukano et al. The paper demonstrate an overall decrease of SPL and a redistribution of Powell's sound sources along the blade surface.*

### **INTRODUCTION**

The design of industrial fans intended for application in mass transit systems is made challenging by an increasingly demanding regulatory framework. The recent European Norm EN 12101-3 requires tunnel ventilation fans to be independently tested and demonstrated to be capable of clearing smoke at elevated temperature in the event of a tunnel fire [1]. The further incorporation of EN 12101-3 into ISO 21927-3 [2] has made the application a worldwide requirement. The significance of a legal requirement to design tunnel ventilation fans to be capable of routine ventilation and emergency operation to clear smoke in the event of a fire, leads to a more conservative mechanical design, consequently sacrificing the aerodynamic efficiency.

An unintended consequence of the requirements of EN 12101-3 is to reduce fan efficiency during normal operation, and so is in direct conflict with the requirements of Regulation 327 [2], intended to reduce the carbon footprint of tunnel ventilation systems during normal operation. This conflict is within the context of a trend toward railway tunnels and metro systems that are both longer and deeper, as such requiring ventilation fans capable of developing a higher pressure for a given flow rate. The situation is further compounded by a shift towards higher speed trains in railway tunnels

and the use of platform screen doors in metro systems. Both result in a significant increase in the magnitude of pressure pulses imposed upon ventilation fans as a train first approaches and then moves away from the ventilation shaft within which they are situated [3,4].

The legislative requirements combined with shifting market requirements have resulted in the constraints and demands placed upon industrial fan designers becoming significantly more onerous over the past decade. One consequence is that historically conservative empirical and semi-empirical design practices have become progressively out-of-date.

A consequence of a reduction in mechanical safety factors is an increased susceptibility of the design to mechanical failure because of the increased risk that a fan may stall in operation, as such inducing increased unsteady mechanical loads in fan rotating components. Consequently industrial fan designers have an interest in design methodologies that will both enable them to produce aerodynamic designs that do not stall in practical application or that are intrinsically stall tolerant if they do. Within the context of industrial fan design the term “stall tolerant” refers to an aerodynamic design that will induce lower alternating stresses in a fan rotating components during stalled operation.

To this aim we have studied the possible application to axial flow fans of sinusoidal leading edges. Originally developed by a biomimicry approach derived from the flippers of humpback whales, we found that [5,6] a sinusoidal leading edge at the tip of the blade allowed to control tip separation.

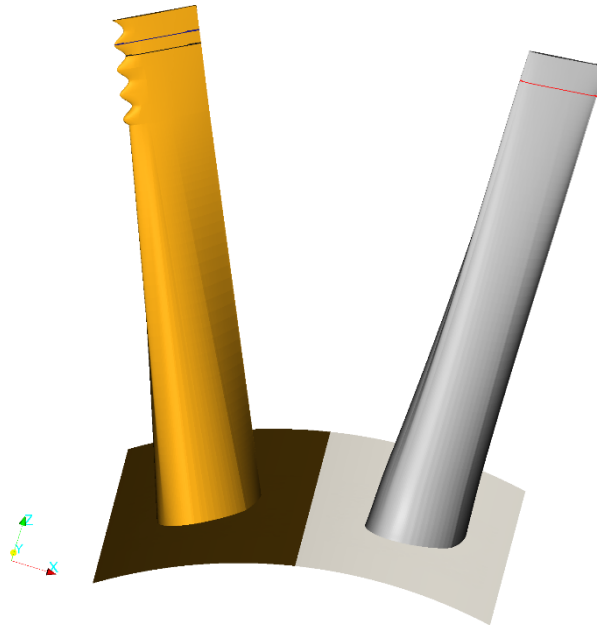


Figure 1: Three-dimensional computer aided design models of the JWFM224 fan blade (left) and the JFM224 fan blade (right).

Here we focus on the acoustic effects of the sinusoidal leading edge, to assess how the geometry performs with this modification.

## THE JFM224 AND JWFM224 FANS

In this paper we assess the acoustic performance of the datum geometry of JFM224 fan and its modified variant, JWFM224, Figure 1. The datum fan is a large fan for tunnel and metro ventilation systems. It is characterized by a rotating speed of 1500 rpm, an external diameter of 2240 mm, hub-to-tip ratio 0.5 and 16 blades, with a 6.5% of tip clearance. Such high value of tip clearance has to be associated to the certification, that requires the fan to operate in event of fire with a 400°C temperature. The modified JWFM224 blade is characterized by a sinusoidal leading edge on the upper 20% of the span of the blade, designed to control separation and stall [5].

This blade was found in [5] to be able to change the dynamics of stall of the datum geometry, altering the pressure developing capability of the fan and its efficiency. To summarise it was found that such leading edge geometry flattened the pressure rise characteristic curve of the fan increasing the pressure in stalled operations, while decreasing it in the stable region of operations. Efficiency curve showed an similar trend, with increase of efficiency at low (stalled) flow rates and decrease at high flow rates.

## NUMERICAL TECHNIQUE

The computational analysis of the baseline and whale-fan was undertaken using the open source finite volume CFD code OpenFOAM 2.3.x written in C++ [7]. The code solved the Unsteady Reynolds-Averaged Navier-Stokes (URANS) incompressible equations in the rotating frame of reference. The turbulence closure used in the present simulation was the non-linear  $k$ - $\epsilon$  model in its cubic formulation with a low-Reynolds number integration [8]. The cubic eddy viscosity model was used to partially account for the anisotropy of the Reynolds stresses and in so doing give better performance in impingement and recirculating regions and additionally partially account for streamline curvature over surfaces. The robustness of this approach when analysing the blade to blade flow field of industrial fan with similar Reynolds and Mach numbers has been established by other scholars who have conducted both benchmarking exercises [9] and also applied the approach in fully three dimensional blade design applications [10, 11]. A common conclusion was that the approach reproduces well three dimensional flow structures, and is therefore inherently suitable for predicting the flow field features induced by the presence of the sinusoidal blade leading edge profile.

The suitability of the chosen numerical approach was specifically considered by Corsini *et al.* [10, 11] who observed that the formulation models eddy viscosity as a third order function of the rate of strain. In so doing the modelling approach overcome the classical limits of the  $k$ - $\epsilon$  turbulence model, minimizing the tendency for overproduction of  $k$  in impingement zones and separation flow regions [9].

The numerical solution is based on the use of a CDS (Central Difference Scheme) to discretize the convective terms into momentum equations, whereas for  $k$  and  $\epsilon$  equations QUICK scheme was selected. The non-linear algebraic equations were solved using Conjugate Gradient solver for all the computed quantities setting convergence tolerance to  $10^{-6}$ .

### Computational grid and boundary conditions

The computational analysis simulated the flow field around a single blade, with periodic boundary conditions imposed at mid-pitch. Only a single blade was analyzed as the focus of the reported research was the effect of the sinusoidal leading edge profile. The computational domain extended one blade chord upstream of the blade leading edge and two blade chords downstream of the blade trailing edge. The computational grid used for both the baseline and whale-fan computational analysis contained 7.1 million hexahedral degrees of freedom. The blade cross-section was divided using 200 cells, with 250 cells used to represent the blade span, Figure 2. The blade aerofoil was enveloped in 80 layers of hexahedra cells. The blade tip region was modelled using 31 cells radially in the blade tip-to-casing region, with 40 cells in the pitch-wise direction. The mesh refinement is such that the average values of the normalised wall distance  $y^+$  are 1.1 on the blade surfaces and 1.3 on the end-walls.

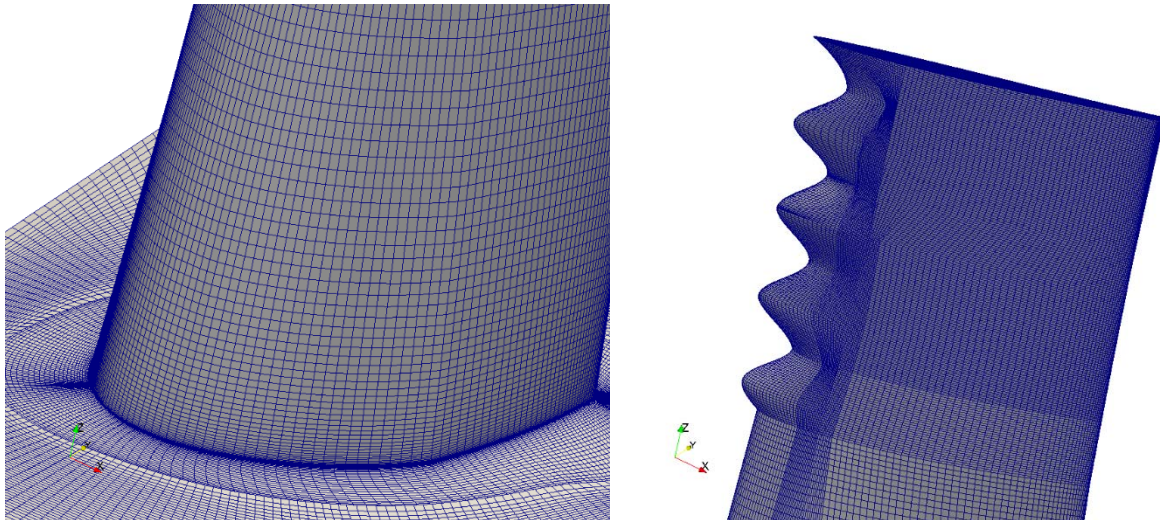


Figure 2. Details of the JWFM224 mesh near the hub (left) and tip (right).

Following the method of Sheard *et. al.* [12] the inflow profiles for both velocity and turbulence levels were derived by numerically simulating the flow field in the fans inlet spinner cone region. Table 2 summarizes the complete set of the boundary conditions on each sub-set of boundary surface.

Table 1 - Boundary conditions

Inflow	velocity, k and $\varepsilon$ profiles [12]
Outflow	Convective
Hub and blade	no-slip condition with zero relative velocity
Casing	no-slip condition with relative velocity $w = -\omega R_{cas}$

## RESULTS

Validation of numerical results was carried out against available JFM224 fan performance measurements. Results are summarised in Table 2, where it total pressure rise and efficiency are listed for available experiments on JFM224 and CFD on the same fan, as well as for CFD of JWFM224. First, the discrepancy between experiments and CFD is within the measurement accuracy, confirming that the numerical setup is able to correctly predict the duty point of the fan. Second, these results confirm those in [5], predicting a 4% loss in total pressure rise for the JWFM224 with respect to the datum geometry and an increase in 0.3% of efficiency.

Table 2 – Aerodynamic performance validation

Total pressure rise [Pa]			Efficiency		
<i>JFM224</i>	<i>JFM224</i>	<i>JWFM224</i>	<i>JFM224</i>	<i>JFM224</i>	<i>JWFM224</i>
<i>EXP</i>	<i>CFD</i>	<i>CFD</i>	<i>EXP</i>	<i>CFD</i>	<i>CFD</i>
2752	2732	2621	69.2 %	69.2 %	69.5 %

With respect to the acoustic performance of the blades, the Sound Power Level (SWL) and Sound Pressure Level (SPL) of the blade was calculated according to Fukano et al. [13] and its reported in Table 3. The blade with the sinusoidal leading edge performs better than the datum geometry, showing a reduction of SWL of -2.3 dB.

Table 3 – Aerodynamic performance [13]

	<i>JFM224</i>	<i>JWFM224</i>
	<i>CFD</i>	<i>CFD</i>
SWL	95.2 dB	92.9 dB

So the overall effect of the sinusoidal leading edge is to induce a reduction of SWL. Yet to understand how this reduction is distributed along the span of the blade, in Figure 3 the SPL for both datum and modified geometries is shown. This figure shows that the sinusoidal leading edge at the tip of the JWFM224 blade results in a redistribution of the SPL along the span. In particular, with respect to the datum JFM224 geometry, there is a noticeable increase of SPL at the hub, up to 20% of the span. At higher radii, on the contrary, the effect of the sinusoidal leading edge is to provide a reduction of SPL up to the tip. The sudden increase at the tip both blades can be ascribed to the effect of the tip leakage vortex and it is worth highlighting that the control effect on the aerodynamics of the blade of the sinusoidal leading edge, results in a reduction of SPL.

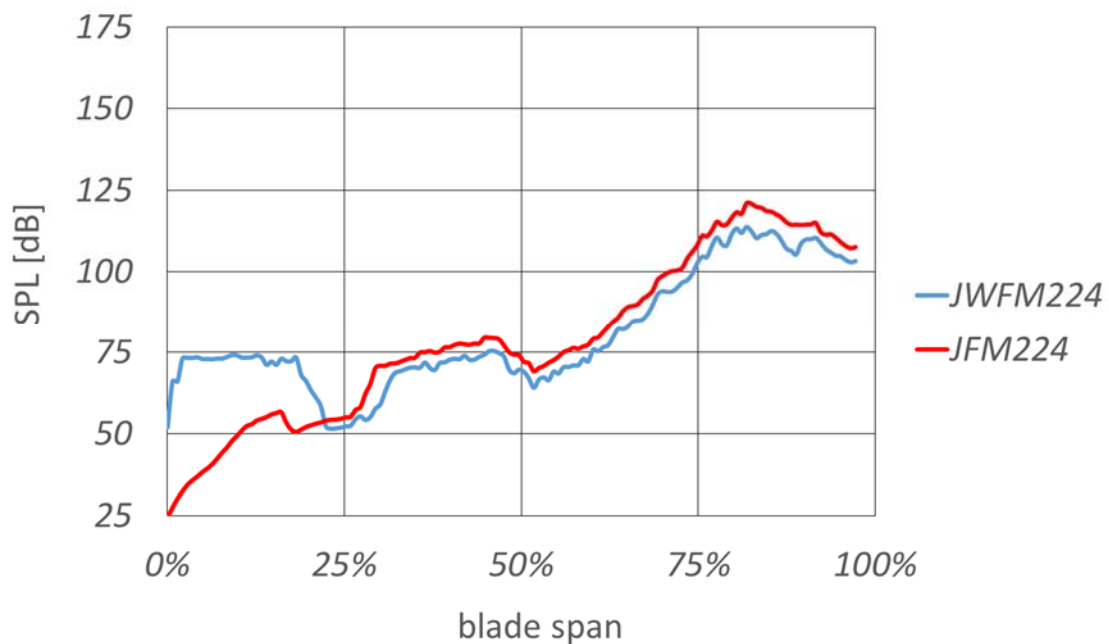


Figure 3. Spanwise distribution of SPL (Fukano et al., 1977), for the JWFM224 (blue) and JFM224 (red) blades.



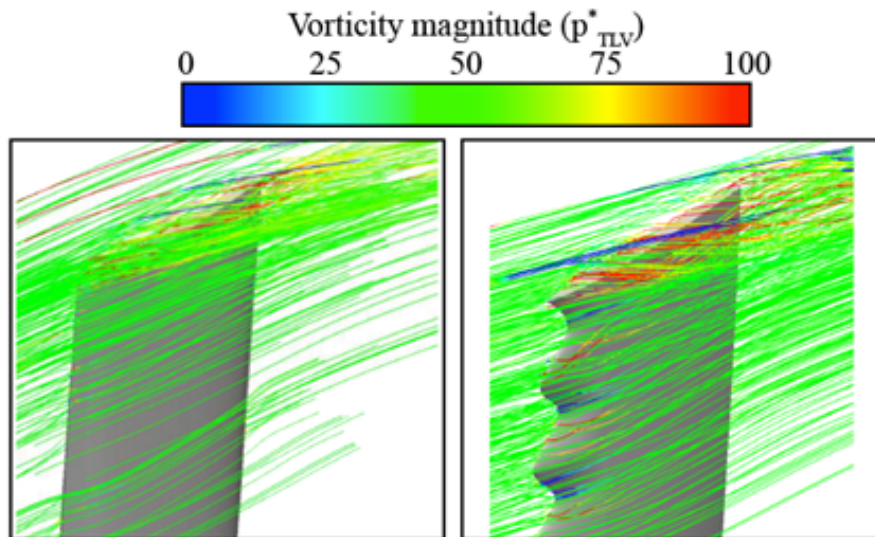


Figure 4. Streamlines colored with vorticity near the tip of the JFM224 (left) and JWFM224 (right) blades.

The control effect of the sinusoid is shown in Figure 4. At this operating point of the fan the sinusoidal leading edge results in an increase of the swirl of the tip leakage vortex, and therefore in an increase of mixing of the vortex, even if the overall aerodynamics of the blade is not affected as the vortex develops in the same position with respect to the datum geometry.

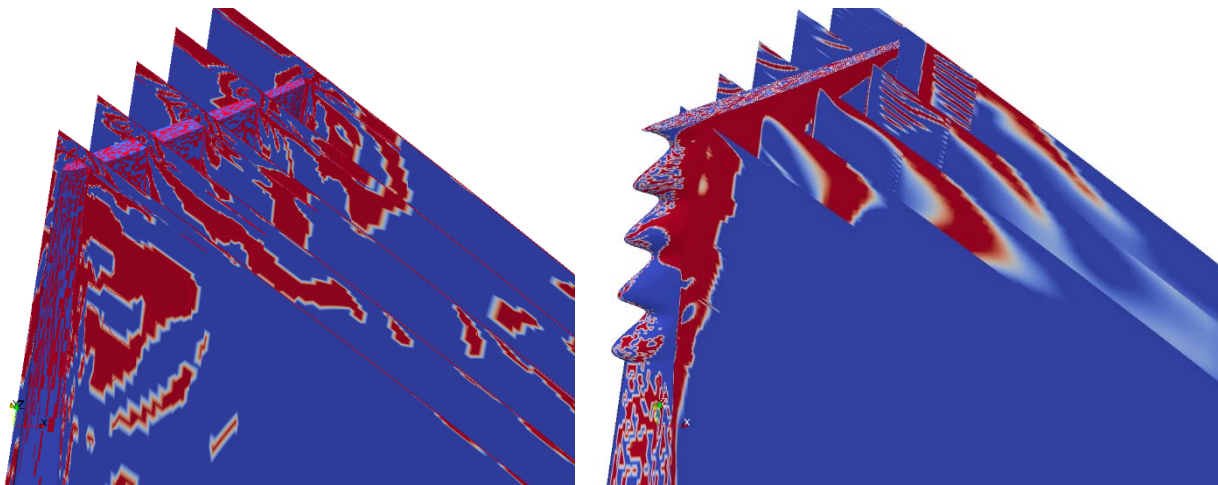


Figure 5. Powell's sound sources near the tip of the JFM224 (left) and JWFM224 (right) blades.

The effect of higher swirl in the tip region of the JWFM224 with respect to the datum JFM224 geometry in terms of acoustic performance of the blades is shown in Figure 5, where Powell's sound sources [14] are shown in red in 5 planes near the blade of the fans. The datum geometry (left) shows that the sound sources are localized near the suction surface of the blade, and convected downstream with the tip leakage vortex. On the contrary, the blade with the modified geometry is characterized by sources at the leading edge near the bumps that are not simply convected downstream, but also are ironed out and roll away from the suction surface.

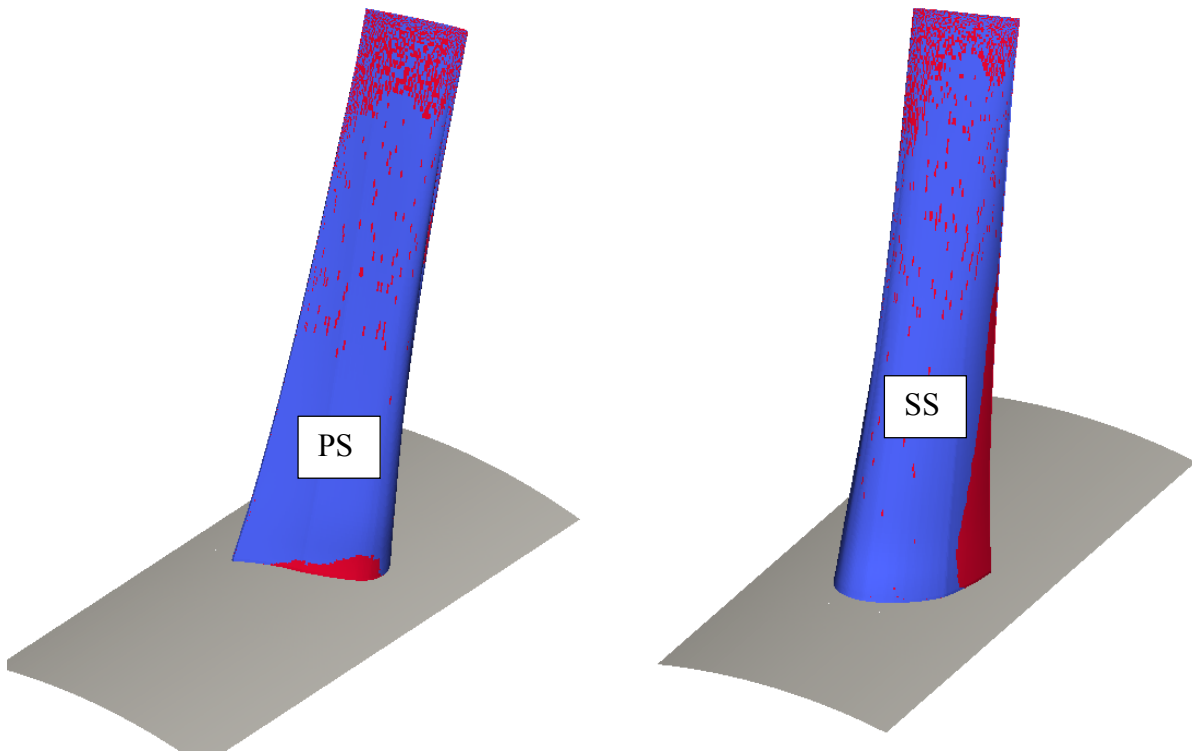


Figure 6. Powell's sound sources near the JFM224 blade surface. Left: pressure side. Right: suction side.

In Figure 6 and Figure 7 Powell's sound sources over the blade are shown respectively for the JFM224 and the JWFM224. For the datum geometry the sources are localized at the tip of the blade for the upper 20% of the span and at the trailing edge on the suction surface for the lower half of the blade.

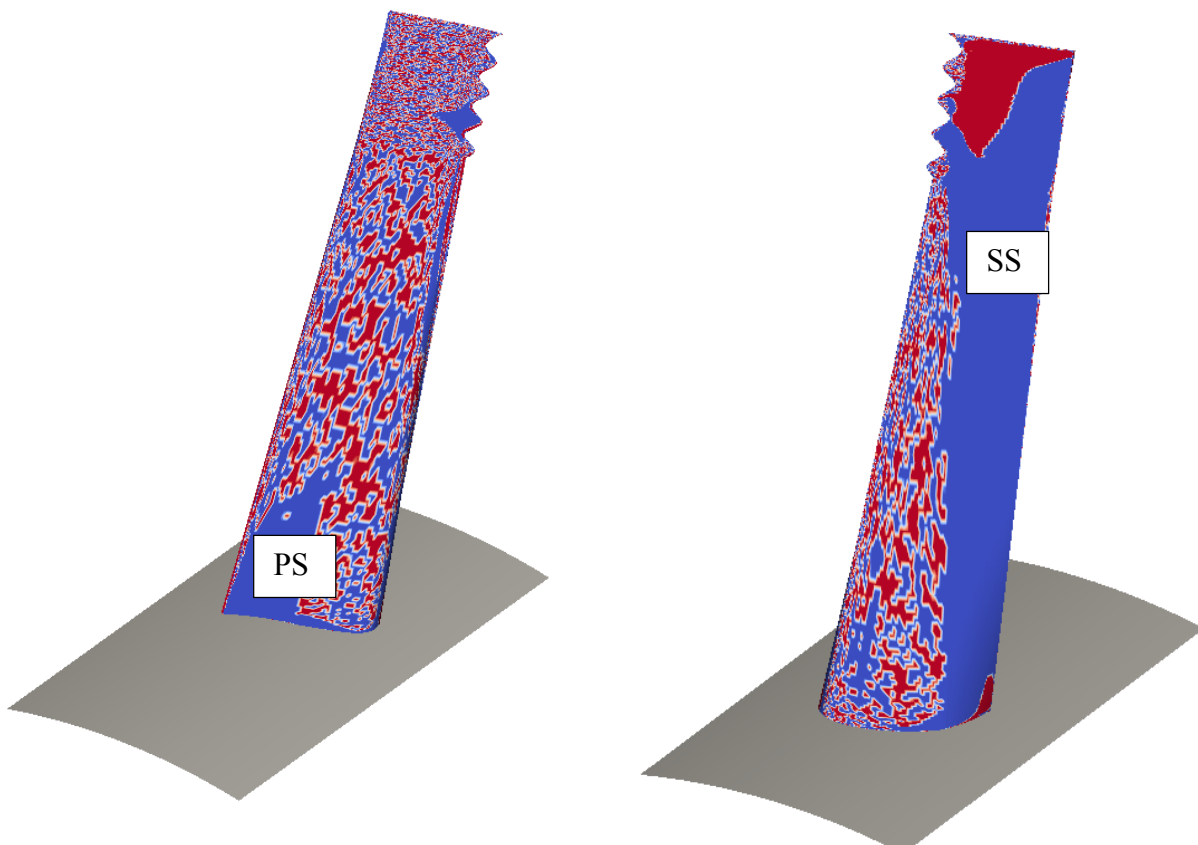


Figure 7. Powell's sound sources near the JWFM224 blade surface. Left: pressure side. Right: suction side.

Completely different figures are shown on the JWFM224 with the modified geometry. In particular sources are localized on the whole leading edge of the blade, and onto the whole pressure surface of the blade. This confirms that even if the modification of the leading edge of the JWFM224 is localized at the upper 20% of the blade span, the redistribution of performance affects the whole blade. This spanwise effect was already observed in [5] when analyzing the pressure distribution onto the blades of the datum and modified geometries.

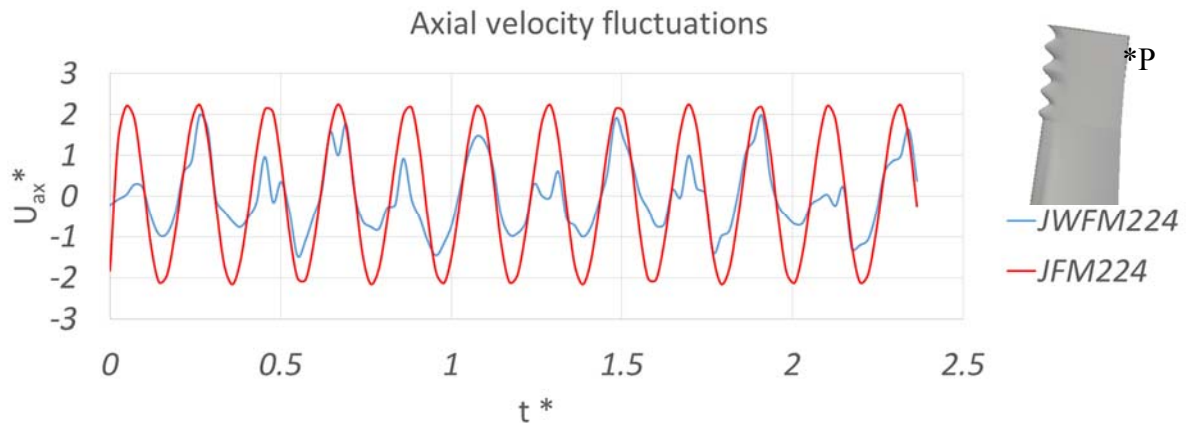


Figure 8. Normalised axial velocity fluctuations near the trailing edge of the blade (see insert) for the JWFM224 (blue) and JFM224 (red)

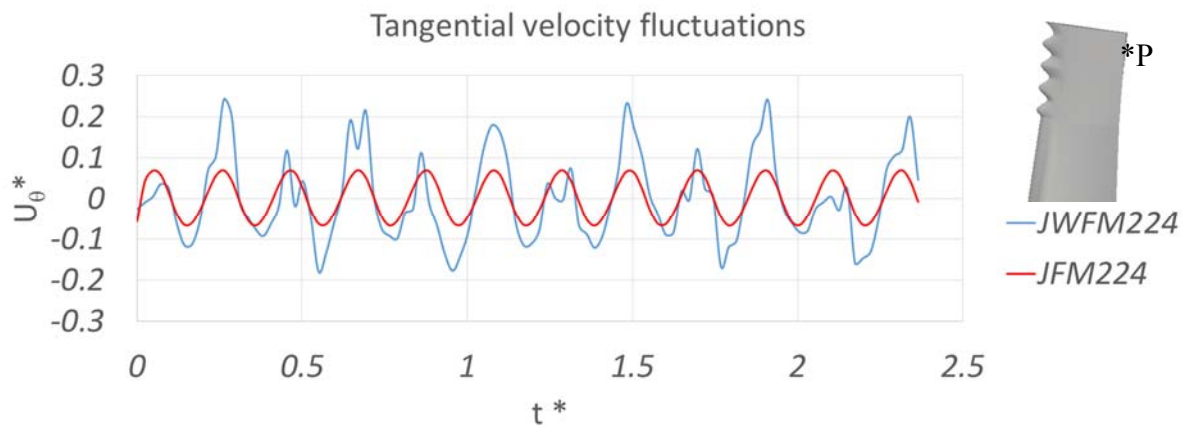


Figure 9. Normalised tangential velocity fluctuations near the trailing edge of the blade (see insert) for the JWFM224 (blue) and JFM224 (red)

A final characterization of the effects of the sinusoidal leading edge is given in Figures 8 and 9 in terms of punctual fluctuations of the axial and tangential velocity components. Velocity signals were acquired at 95% of the blade span near the suction surface at the trailing edge and are here normalized with respect to the tip velocity of the fan. While the JFM224 shows a periodic signal with a frequency equal to the Blade Passing Frequency (BPF), the signal of the JWFM224 has a bimodal characterization due to the vorticity shed by the sinusoidal leading edge, that results in two peaks corresponding to the BPF and twice the BPF.

## CONCLUSIONS

Taking a lead by a previous aerodynamic characterization of the performance of a modified sinusoidal leading edge, derived by biomimicry assumptions, the acoustic effects of this modifications were assessed on an axial fan for tunnel and metro ventilation systems.



Analysis of SWL showed that the modified leading edge results in a reduction of 2.3 dB of the overall SWL. A more detailed analysis of data allowed to separate the effects of this reduction, highlighting that the hub of the modified geometry is characterized by higher SPL, but that the rest of the blade is affected by an overall reduction of noise.

Tip effects were discussed showing how the increase in mixing of the tip leakage vortex in the JWFM224 lead to an reduction of Powell's sound sources.

The same analysis of Powell's sound sources showed a complete redistribution along the blade surface, further confirming that even if the sinusoidal leading edge is applied only on the upper 20% of the blade span, the whole blade is affected.

Tip effects were finally discussed in terms of velocity fluctuations at the trailing edge. The effects of the sinusoidal leading edge were to pass from a velocity signal characterized by the BPF, to one with two peaks corresponding to the BPF and twice the BPF.

## BIBLIOGRAPHY

- [1] A. G. Sheard and N. M. Jones - *Powered smoke and heat exhaust ventilators: the impact of EN 12101-3 and ISO 21927-3*. Tunn Undergr Sp Tech, vol. 28: 174-182, **2012**.
- [2] A. G. Sheard AG and N. M. Jones - *Approval of high-temperature emergency tunnel-ventilation fans: the impact of ISO 21927-3*. In: Proceedings of the ITA–AITES world tunnel congress and 34th general assembly, Agra, India, 19–25, pp. 1817–1826, **2008**.
- [3] L. Cardillo, A. Corsini, G. Delibra, F. Rispoli, and A. G. Sheard - *A numerical investigation into the aerodynamic effect of pressure pulses on a tunnel ventilation fan*. Proceedings of the Institution of Mechanical Engineers, Part A: Journal of Power and Energy Volume 228 Issue 3, pp. 284 – 298, May **2014**.
- [4] D. Borello , A. Corsini, G. Delibra, M. Fiorito, A. G. Sheard - *Large-Eddy Simulation of a Tunnel Ventilation Fan*. J. Fluids Eng. Vol. 135(7), **2013**.
- [5] Corsini, A., Delibra, G, and Sheard, A.G., 2014, The application of sinusoidal blade-leading edges in a fan-design methodology to improve stall resistance, Proceedings of the Institution of Mechanical Engineers, Part A: Journal of Power and Energy May 2014 vol. 228 no. 3 255-271, 10.1177/0957650913514229
- [6] A. Corsini, G. Delibra and A. G. Sheard - *On the role of leading-edge bumps in the control of stall onset in axial fan blades*. J Fluid Eng. Vol 135, **2013**.
- [7] H.G. Weller, G. Tabor, H. Jasak - *A tensorial approach to continuum mechanics using object-oriented techniques*. Comput Phys vol. 12, **1998**.
- [8] F. S. Lien and M. A. Leschziner - *Assessment of turbulence-transport models including non-linear RNG eddy-viscosity formulation and second-moment closure for flow over a backward-facing step*. Comput Fluid vol. 23: 983–1004, **1994**.
- [9] B. Durbin - *Review: adapting scalar turbulence closure models for rotation and curvature*. J Fluid Eng vol. 133, **2011**.
- [10] A. Corsini, F. Rispoli, A. Santoriello and T. E. Tezduyar - *Improved discontinuity-capturing finite element techniques for reaction effects in turbulence computation*. Comput Mech vol. 38: 356–364, **2006**.
- [11] A. Corsini and F. Rispoli - *Flow analyses in a high-pressure axial ventilation fan with a non-linear eddy viscosity closure*. Int J Heat Fluid Flow vol. 17: 108–155, **2005**.

- [12] A. G. Sheard and A. Corsini - *The mechanical impact of aerodynamic stall on tunnel ventilation fans*. Int J Rotating Mach vol. **2012**.
- [13] T. Fukano, Y. Kodama and Y. Senoo – *Noise generated by low pressure axial flow fans, I: modeling of turbulent noise*. Journal of Sound and Vibrations vol. 50 (1), pp. 63-74, **1977**.
- [14] A. Powell – *Theory of vortex sound*. J. Acoust. Soc. Am. Vol. 36, 177, **1964**.